CrossMark

ORIGINAL ARTICLE

Dynamics in Polysaccharide Glasses and Their Impact on the Stability of Encapsulated Flavors

Ekneet K. Sahni[1] · Meena Thakur[2] · Michael A. Chaney[3] ·
Gregory Sherman[3] · David Paul Siegel[3] · Michael J. Pikal[1]

Abstract The aim of this work is to examine the correlation between measured instability of model flavor compounds in glassy matrices with the calorimetric relaxation times of the matrices. Spray-dried carbohydrate matrices were chosen as the model compounds for this study. Enthalpy relaxation times were determined for spray-dried carbohydrate matrices using differential and isothermal calorimetric methods. The losses of the volatile methyl acetate, ethyl acetate and limonene, as well as formation of limonene oxidation products, were measured by gas chromatography. Storage conditions were 30 and 40 °C, with samples equilibrated with 11, 23, 33 and 43 % RH at each temperature. A comparison of the relaxation times for temperatures below Tg was made using Modulated DSC (MDSC) and a Thermal Activity Monitor (TAM). TAM yields significantly lower values for relaxation times implying that it is capturing some of the faster dynamics as well as dynamics that are activated near Tg. However, plots of relaxation times as determined by both techniques versus temperature appear to converge at Tg. An increase in the relative humidity results in moderately higher loss of volatiles (methyl acetate, ethyl acetate and limonene) and greater oxidation rates. In general, there is a good correlation between relaxation time and stability, with greater enthalpy relaxation time associated with better stability. Enthalpy relaxation time appears to be a useful predictor of stability for both loss of volatiles and oxidation of limonene.

Introduction

Flavors are complex mixtures of natural or synthetic chemicals, which are subject to loss by evaporation, degradation via chemical reaction with oxygen or water, or nearly irreversible binding to other components of foods. A variety of technologies are used to encapsulate them to increase their shelf stability [1–4]. A widely used method of encapsulation is spray drying [5]. The flavor is dispersed as a solution or emulsion in a concentrated suspension of carrier material, which is then atomized and rapidly dried. The carrier material is often a mixture of polysaccharides and/or oligosaccharides, which dry to form a glassy matrix. To protect the encapsulated flavor, the dried carrier must be poorly permeable to volatile flavor components and to oxygen. It has long been known that carriers containing a mixture low and high molecular-weight polysaccharides, or a single modest average molecular-weight polysaccharide, provide stability to encapsulated flavor; and that the carrier must be below the glass transition temperature to prevent excessive flavor degradation [6–10]. The favorable barrier properties of such mixtures have often been attributed to their high density relative to high molecular weight polysaccharides, and more recently to their lower average molecular-scale defect size [11, 12]. Presumably, the rate of transport of gasses and flavor molecules through glassy

✉ David Paul Siegel
david.siegel@givaudan.com

[1] Department of Pharmaceutical Sciences, School of Pharmacy, University of Connecticut, 69 N Eagleville Road, Unit 3092, Storrs, CT 06269, USA

[2] Onyx Pharmaceuticals, Inc., 249 E. Grand Avenue, South San Francisco, CA 94080, USA

[3] Givaudan Flavors Inc., 1199 Edison Drive, Cincinnati, OH 45216, USA

matrices is related to the dynamics of motions on different length scales, in a fashion analogous to the relationship between encapsulated protein stability and matrix dynamics in amorphous pharmaceuticals and freeze-dried pharmaceutical delivery systems. [13–18] However, we are unaware of reports relating the time scales of matrix molecular mobility directly to the rate of encapsulated flavor degradation, where degradation is defined as the loss of small molecular-weight, volatile components such as methyl acetate, and oxidation of an encapsulated small molecular-weight encapsulated compound (limonene). The objective of this study is to relate the measured loss rates of model flavor compounds from glassy matrices under controlled conditions to the micro-calorimetric relaxation times of the same matrices. We seek only semi-quantitative relationships, to see if more work relating different relaxations of the matrices to flavor degradation is warranted.

The glassy system upon aging experiences an increase in the relaxation time and hence a decrease in the molecular mobility. As the system moves toward equilibrium below T_g, the energy and free volume decreases and the structural order increases. This process is called structural relaxation. Various macroscopic properties of glassy materials change during physical aging other than energy and free volume, such as refractive index, electrical conductivity and viscosity [19]. Many techniques, such as differential scanning calorimetry [20, 21], modulated differential scanning calorimetry [22–24], dielectric thermal analysis [25], dynamic mechanical thermal analysis [26–29], are employed to study the structural relaxations in amorphous systems focused on temporal variation of the above-mentioned macroscopic properties which in turn may affect the stability of flavors encapsulated within amorphous solids. Hence, finding a correlation between the destabilization mechanism in flavor delivery systems and enthalpy relaxation would be useful in better understanding the stability behavior and therefore facilitate design of a more stable matrix.

Materials and Methods

Materials

Spray dry matrix components were obtained as follows: octenyl succinate modified starch (Capsul®) was obtained from Ingredion Corporation, maltodextrin (10 DE) from Grain

Processing Corporation, and sucrose from Dominos. All extraction solvents were GC grade and obtained from Fisher Chemical Co. Alpha-Amylase was obtained from human saliva (CAS #9000-90-2) and was obtained from MP Biomedicals, Santa Ana, California, USA.

Methods

Spray Drying

The composition of the spray-dried matrices is shown in Table 1. The model flavor was composed of methyl acetate, ethyl acetate and limonene 86.7/6.67/6.67 w/w/w. Spray dry emulsions were made by making 50 % by weight total solids (including either 15 % of the model flavor or no flavor for "blank" samples) in water by homogenization, and were preheated to 40 °C. These emulsions were introduced into an Anhydro PSD55 dryer (with a wheel atomizer operating at 35,000 rpm) with dry input air at a feed rate of 300 g/min. The inlet and outlet temperatures were 180 and 90 °C respectively. The initial flavor contents of the dry powders determined by gas chromatography (below) were 0.26 %/ methyl acetate, 0.40 % ethyl acetate, and 13.8 % limonene for the 50 % sucrose sample; and 0.26 % methyl acetate, 0.43 % ethyl acetate and 13.6 % limonene for the 30 % sucrose sample, by weight of the dry powders. The average mean volume particle size as determined using a CILAS 1190 laser size analyzer was 37.8 and 26.2 μm for the 50 % sucrose and 30 % sucrose powders; respectively.

Stability Studies

The loss of the volatile methyl acetate, ethyl acetate and limonene, along with the buildup of limonene oxidation products, was measured periodically by gas chromatography on extracts of the samples. The storage temperatures and relative humidity was 30 and 40 °C, with chambers at 11, 23, 33 and 43 % RH at each temperature. Battery operated fans were added to the chambers to speed equilibration, and the chambers were not evacuated to accelerate equilibration (as this would remove oxygen that must be present in order to judge the efficacy of the matrices in preventing oxidation of encapsulated flavors). The ambient conditions were close to, or above, the glass transition temperature in some instances. To ensure uniform

Matrix	Component			Wight ratio
50 % Sucrose	MaltrodextrinDE10	Capsul (modified starch)	Sucrose	4:1:5
30 % Sucrose	MaltrodextrinDE10	Capsul (modified starch)	Sucrose	6:1:3

Table 1 Composition of the spray-dried carbohydrate matrices

sampling of partially caked powder, the samples were disposed as layers no more than 2 mm thick on small watch glasses, so that the entire sample could be extracted with the solvent subsequent to equilibration. The chambers must be opened to retrieve samples, and then reclosed for re-equilibration. In our experience inclusion of fans in the chambers reduces the equilibration times to several days. This interval is several times smaller than the interval between sampling points. Therefore, to a first approximation, we neglect the influence of the short re-equilibration time on the overall aging times.

Gas Chromatographic Method

Extractions All solvents were GC grade. The extraction procedure for quantification of ethyl acetate, limonene and limonene oxidation byproducts was as follows. 0.50–1.00 g of dry sample were weighed into tared centrifuge tubes. 20 mg of α-amylase was added to each, followed by 3 to 4 drops of chlorocyclohexane as an internal standard. Then 4 ml of water was added to each tube, followed by vortex mixing for 1 min. The samples were allowed to stand for 1–2 h at room temperature. Then 20 mL of acetone was added to each tube, followed by vortex mixing for 1 min. The tubes were then placed on a shaker table for 1 h. Then 5–10 g of sodium sulfate was added to each tube. Each tube was shaken well and allowed to stand for a further hour. The extracts were then transferred to 2.5 mL G.C. autosampler vials.

The extraction procedure for quantification of methyl acetate was different from the one above. (This is due to interference of acetone solvent with the methyl acetate peak in subsequent GC.) The procedure was the same as the one above up through addition of the chlorocyclohexane. Thereafter, 8 ml of water was added to each tube followed by vortex mixing for 1 min, and the tubes were allowed to stand at room temperature for 1–2 h. Then 10 mL of pentane was added to each, followed by 1 min of vortex mixing. The tubes were placed on a shaker table for 1 h. 5 g of sodium chloride was added to each tube. The tubes were shaken well and allowed to stand for a further hour. If necessary, the tubes were centrifuged to separate the clear solvent layer. The top (solvent) layers were then transferred to 2.5 mL G.C. autosampler vials.

Analysis Samples were analyzed using an Agilent 7683 GC with FID detection , using a Stabilwax column, 30 m in length, 0.53 mm ID, 1 μm d_f; through a Split/Splitless port at 250 °C, 4.0 psi, 5.9 ml/min purge flow, using a 1.00 min purge time, 14.8 ml/min total flow, split injection of 5 μl. The temperature ramp used started at an initial oven temperature of 32 °C, ramping at 10 °C/min. to 240 °C. Response was calibrated using appropriate standard solutions. The weight of total oxidation products was assessed as the total content of limonene oxide, carveols and carvone.

Water Activity Control (Samples for Calorimetric Analysis)

Samples were stored in small glass bottles at different water activity (a_w) conditions. This was accomplished by equilibrating the sample in a desiccator containing saturated salt solution of known RH values of 11 % (lithium chloride), 23 % (potassium acetate), 33 % (magnesium chloride), 43 % (potassium carbonate) under vacuum at room temperature for at least a month. Humidity equilibration was stopped after no further weight gain was observed for each sample.

Karl Fisher Analysis

Moisture content in the sample was measured using a Karl Fisher Moisture Analyzer (Metrohm, KF756). Samples were suspended in 3 mL of dry solution (Ethylene glycol: methanol, 80:20) and 0.5 mL of solution was injected into the titration cell. The amount of water in the dry solution was obtained from a blank reading, which was subtracted from the sample reading. Thus, knowing the amount of water content and the weight of the sample, the % residual (w/w) water content in the sample was determined.

Thermal Gravimetric Analysis

Moisture content of the sample was also determined using a thermal gravimetric balance (TGA, Q5000, TA instrument). Each sample (10–15 mg) was analyzed in an open aluminium pan attached to the microbalance over the temperature range, 25–500 °C, using a scanning rate of 10 °C/min. At the end of the experiment, loss in weight was used to calculate the moisture content of the sample. Measurements were carried out in duplicate. The TGA module was calibrated using a nickel standard.

Specific Surface Area Measurement

The specific surface area measurement of the dried sample was measured using a BET-specific surface area analyzer Flowsorb II (Micromeritics Instrument Corporation, Norcross, GA). Samples were degassed for 2 h at 40 °C by passing a stream of inert gas mixture of helium and krypton through the sample. The instrument was calibrated using 100 % krypton under room conditions. After the sample was dried, single point adsorption of krypton was carried out by placing the sample holder in liquid nitrogen and flowing the He-Kr gas mixture over the sample. To characterize the amount of krypton adsorbed, the sample holder was immersed in a water bath at room temperature to desorb the krypton.

Polarized Light Microscopy

Micrographs of the blank matrices were taken using Zeiss microscope (equipped with a polarizer) equipped with Sony color video camera (CCD-IRSI/RGD, Japan) at room temperature. A 40× objective was used. Samples were placed on untreated slides and covered with untreated cover slips. Immersion oil (Cargille A) was used to disperse the sample before taking the micrographs.

Hot stage Microscopy

The sample was dispersed using immersion oil (Cargille A) on a untreated slide and covered with untreated cover slips. Sample was heated on a Linkam LTS350 stage. A Linkam CI94 microscope (containing a polarizer), which is equipped with Olympus camera, was used to take picture every 60 s. A 40× objective was used.

Calorimetric Measurements

Isothermal microcalorimetry was the instrument of choice to evaluate relaxation times as it directly measures the rate of energy change during annealing with very high sensitivity, thereby even permitting very slow processes to be probed effectively [30]. However, modulated DSC can also be used to evaluate the time dependence of enthalpy relaxation by measuring the enthalpy recovered near the glass transition as a function of annealing time. So both methods were used and compared. As will be demonstrated, results are qualitatively the same but significant quantitative differences are observed.

Modulated Differential Scanning Calorimetry

Enthalpy recovery experiments were conducted using a DSC Q1000 from TA instruments (New Castle, DE) equipped with refrigerated cooling system in its modulated mode. For use in the modulated mode, the instrument was calibrated for temperature using high purity indium and for heat capacity with sapphire. The following modulation parameters were used: amplitude±0.5 °C, frequency 60s and heating rate 1 °C/min. An empty pan was used as reference. Approximately 5–10 mg of sample was compacted to a thin disc and placed in the hermetically sealed aluminum pans for analysis. Since the blank samples were equilibrated at various relative humidities, all sample handling for DSC was done in a glove bag maintained at respective relative humidity as that of the sample.

The glass transition temperature was determined as the midpoint of the step change in reversing heat capacity at T_g (determined using Universal Analysis Software, TA Instruments, version 4.7A). In order to measure enthalpy recovery, the sample was first heated above T_g and annealed at that temperature for 3–5 mins in the hermetically sealed pan to remove its thermal history [30]. This was followed by quenching and subsequent annealing process where the samples were annealed for various time points in the DSC at various annealing temperatures (as shown in Tables 3 and 4), followed by the subsequent heating scan measurement to evaluate the enthalpy recovery from the non-reversing modulated DSC signal, as described by Kawakami & Pikal [30].

For relaxation studies, the decay or relaxation function Φ (t, T) was determined using Eq. (1) from the enthalpy recovery at any given time t (assuming the measured recovery is equal to the corresponding enthalpy relaxation):

$$\Phi(t,T) = 1 - \frac{\Delta H(t,T)}{\Delta H(\infty,T)} \tag{1}$$

where, $\Delta H(t,T)$ is the enthalpy recovery determined by integrating the area under the non-reversing peak obtained after annealing the sample at temperature T for time t in hours.

Below the glass transition, amorphous solids exist as non-equilibrium liquids with extremely high viscosities ($>=10$ [12]Pa.s) [31]. Therefore they relax constantly but slowly towards equilibrium at a characteristic rate, eventually reaching a maximum enthalpy change equal to $\Delta H(\infty,T)$ the value of which can be calculated using the following relation:

$$\Delta H(\infty,T) = \Delta C_p\left(T_g - T\right) \tag{2}$$

where, ΔC_p is the heat capacity change at the glass transition temperature T_g and T is the temperature of annealing.

The following Kohlrausch–Williams–Watts (KWW) stretched exponential expression has been used extensively to describe the complex kinetics of enthalpy relaxation in glassy materials during aging: [20, 30, 32, 33]

$$\Phi(t,T) = \exp\left[-\left(\frac{t}{\tau}\right)^{\beta}\right], 0 < \beta \le 1 \tag{3}$$

In the above equation $\Phi(t,T)$ is the relaxation function calculated using Eq. (1), t is the time in hours, τ is the relaxation time in hours, and β is the stretched exponential parameter representing the distribution of relaxation times. The value of β ranges from 0 to 1; with values approaching 1 indicate a homogeneously relaxing system and smaller values indicate a wide distribution of relaxation microstates [34]. Relaxation parameters (τ and β) were obtained from the non-linear curve fitting (OriginPro 8.0) of the empirical Eq. (3) to the experimental relaxation function data acquired from Eq. (1). The kinetic model (KWW equation) assumes that the relaxation is a constant and hence independent of time. However, during the aging process, the relaxation time τ increases. Eq. (3) assumes the relaxation time is a constant, independent of time, and the value of β obtained from the fit is a complex average

of the relaxation times over the course of the aging period and does not represent the relaxation time of the initial sample. Moreover, the value of β obtained is also in error; it is too small [30]. However, modeling studies indicate that the value of τ^β obtained from the fit is a good approximation to the initial value of τ^β [30]. Therefore, it is the value of τ^β that is reported, which represents the reciprocal of a "rate constant" defined on a stretched time scale.

In addition to recovering the enthalpy lost during relaxation, the endotherm obtained in the non-reversing signal includes a small contribution due to the "frequency effect", which is essentially an artifact, and would also contain any contribution originating from relaxation during the slow scan to higher temperature. These contributions were eliminated by subtracting the area of the non-reversing peak (apparent enthalpy recovery value) obtained at time (t=0) from all other annealing time points as described in detail by Kawakami & Pikal [30]. As the frequency effect is contingent on the sample size and density [35, 36], consistent sample sizes were used to ensure equal contribution due to the frequency effect. Thus, the data obtained contain only enthalpy recovery that occurs in the vicinity of the T_g.

Isothermal Microcalorimetry (Thermal Activity Monitor)

The exothermic heat associated with the structural relaxation was measured isothermally using a Thermal Activity Monitor (TAM). Unlike MDSC, TAM provides a very sensitive and direct measure of the rate of energy gain or loss as a function of time during annealing [30, 37]. The calorimetric experiments were performed using about 200–250 mg of sample contained in stainless steel ampoules. The spray-dried samples equilibrated at particular humidities were transferred from storage vials to the measuring ampoules in a same humidity glove bag as that of the sample. As the samples were already relaxed, they were pretreated before loading them into the TAM units. That is, the thermal history of the samples was erased by placing the ampoules containing the sample in a sand bath equilibrated at temperatures higher than the glass transition temperature of the sample for 30 min. Next, the sample was quench-cooled in a sand bath equilibrated at 5 °C for 20 min. Crystalline glycine of equivalent weight as

Table 2 Specific Surface areas for 50 and 30 % Sucrose, blank and flavored matrices

Sample	Average specific surface area (m2/g)
50 % sucrose	0.27±0.01
50 % sucrose+model flavor	0.25±0.01
30 % sucrose	0.22±0.01
30 % sucrose+model flavor	0.40±0.01

The standard deviation is for three independent measurements

that of the sample was used as an inert reference. The sample and reference were then placed at the thermal equilibration position in the calorimeter for 30 min, and then lowered into the measurement position. The power output was recorded as a function of time every min for up to 72 h. The first hour data was discarded due to the artifacts related with equilibration of the sample and reference ampoules [30]. A minimum of three samples were tested at any given set of experimental conditions.

The following "modified stretched exponential" (MSE) derivative expression is employed to evaluate the heat power P, μW/g, with time t in hours:

$$P = 277.8 \frac{\Delta H_r(\infty)}{\tau_0} \cdot \left(1 + \frac{\beta t}{\tau_1}\right) \cdot \left(1 + \frac{t}{\tau_1}\right)^{\beta-2} \cdot \exp\left[-\left(\frac{t}{\tau_0}\right) \cdot \left(1 + \frac{t}{\tau_1}\right)^{\beta-1}\right] \quad (4)$$

where, 277.8 is a numerical factor due to conversion of units, τ_0 is a relaxation time constant, τ_1 is a relaxation time constant for the "Short-Time Limit", β is known as the stretch parameter and represents the distribution of independently relaxing substates. $\Delta H_r(\infty)$ is the enthalpy relaxation at time infinity calculated from Eq. (2).

The MSE equation was chosen as it could be used for times approaching time zero as opposed to the KWW equation which predicts the power, P, approaches infinity as time approaches zero, which is unphysical and causes fitting problems. [37] The relaxation parameters (τ_0, τ_1 and β) were obtained from the nonlinear curve fitting of the raw data to Eq. (4) by utilizing OriginPro 8.0. The relaxation time (τ_D) was calculated using the following expression:

$$\tau_D = (\tau_0)^{1/\beta} (\tau_1)^{\frac{(\beta-1)}{\beta}} \quad (5)$$
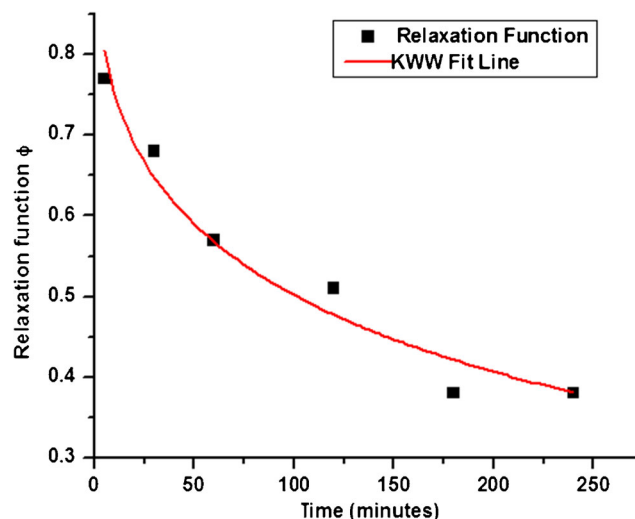

Fig. 1 Shows the relaxation function Φ as a function of time for 50 % Sucrose at 33 %RH and 25 °C as the annealing temperature. The solid line represent the "best fit" values obtained from the KWW equation using the MDSC. The KWW parameters obtained by the fit are: β= 0.39±0.05, τ^β=8.54±1.9 min, χ^2=0.00125
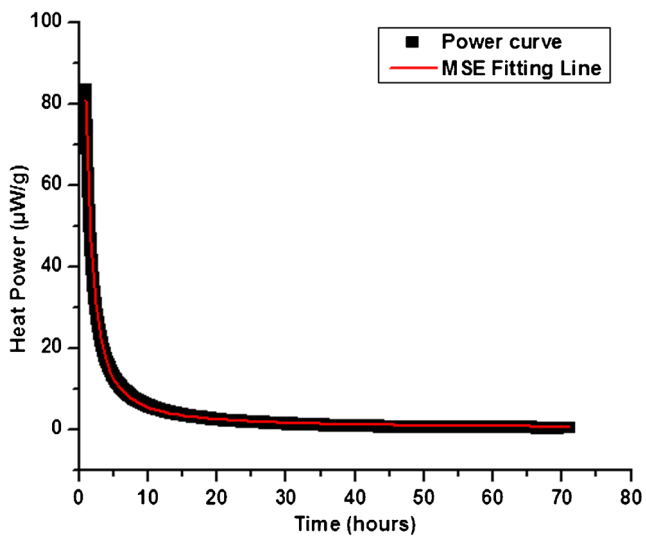
Fig. 2 Power versus time data from an isothermal microcalorimetry for 50 % Sucrose at 33 %RH and 25 °C. The curve was generated by fitting the derivative form of the MSE equation to the TAM data (χ^2=0.00125 (a measure of the goodness of fit), β=0.172±7.07E-4, τ_0=1.81±0.016, τ_1= 0.92±0.008, ΔH_r=2.3 J/g

Note that at long times, the MSE equation reduces to the same form of the KWW equation, where τ_D becomes equivalent to the value of τ in the KWW equation. Due to relaxation induced errors described earlier, which impact evaluations of τ_D and β, we use τ_D^β as the structural relaxation time parameter.

Results and Discussion

Crystallinity, Moisture Content, Specific Surface Area and Thermal Analysis

As a qualitative measure of crystallinity, we characterize birefringence as determined by polarized light microscopy. A non-isotropic system does not produce birefringence so "nominally" the absence of birefringence indicates absence of crystallinity, at least if the potential crystallinity is non-cubic. Birefringence studies were performed where the blank formulation containing 50 % sucrose was equilibrated at 33 % RH, 40 °C for 10 days. To verify that the birefringence was not due to sucrose crystallization, DSC and hot stage microscopy were performed (data not shown). DSC showed a distinct glass transition temperature around 45 °C, likely representing the glass transition of the sucrose-rich phase and a distinct endotherm around 145 °C for the 50 % sucrose blank samples. In order to determine if the 145 °C endotherm was due to melt of sucrose crystals, some crystalline sucrose was added in both 50 % sucrose blank-33 %RH and 50 % sucrose blank-33 %RH, aged at 40°C (10 days). The addition of crystalline sucrose however, didn't increase the area of the 145° endotherm in thermograms but instead introduced a separate endotherm at about 20 °C higher temperature. Thus, in this system,

crystalline sucrose melts at about 165 °C, meaning the 145 °C endotherm represents melting of another component. Hot stage microscopy demonstrates that the birefringence observed during the PLM studies disappears at 145 °C, verifying that the birefringence is not due to sucrose crystallization. By default, the 145 °C endotherm represents a thermal event associated with a formulation component other than sucrose, probably a melt.

The water content for both the systems was determined after the samples were equilibrated at a given humidity for at least a month and no further gain in moisture content was observed. Water content as determined by thermogravimetric analysis for 11, 23, 33 and 43 % is as follows: 3.5±0.6, 4.03± 0.01, 6.28±0.05, 6.92±0.13 respectively for 30 % Sucrose and 3.5±0.2, 5.1±0.6, 5.50±0.03, 5.50±0.03, 6.10±0.03 respectively for 50 % Sucrose. Water content values as determined by Karl Fisher analysis also gave the same trend although gave somewhat higher values particularly at higher humidity of 43 %. The residual water calculated based on literature data for the formulation components was in better agreement with the TGA data than with the corresponding Karl Fischer data (data not included). However, the trend of water content with humidity is semi-quantitatively the same regardless of the source of water content data.

Table 2 shows the comparison of the specific surface area for blank and flavored matrices for 50 and 30 % sucrose. The specific surface areas were very similar for both blank and flavored matrices for 50 % Sucrose. However, 1.5–1.7 fold increase in specific surface area was seen for the flavored 30 % sucrose matrix when compared to the one without flavor. We speculate that this is linked to the density and therefore the retention capacity of flavor components. For the matrix containing 50 % Sucrose, T_g is low enough to allow the system to remain well above the T_g until the water content is quite low. This in turn might facilitate formation of a fairly dense glassy (low porosity) matrix with more capacity to efficiently retain the flavors as compared to 30 % Sucrose. The matrix containing 30 % Sucrose may be permeable enough to permit more extensive vaporization of volatile flavor components within the particle interior during drying. This may further increase the porosity and mechanical fragility of the particles relative to particles without flavor, resulting in an increased specific surface area.

Characterization of Enthalpy Relaxation: Comparison of Isothermal Microcalorimetry with Modulated Differential Scanning Calorimetry

Both modulated DSC and isothermal microcalorimetry were used to evaluate the relaxation times for 50 % sucrose. Although both calorimetric techniques nominally measure the same phenomena, previous work indicates that, at least for simple one component systems, isothermal microcalorimetry

Table 3 Comparison between calorimetric relaxation times (in hours) and beta values in parenthesis, obtained from isothermal microcalorimetry and modulated DSC along with enthalpy relaxation and recovery obtained at four temperatures for 50 % Sucrose at 23 %RH

% RH	Temperature (°C)	Isothermal microcalorimetry (MSE)		Modulated DSC (KWW)	
		Enthalpy relaxed (J/g)	Relaxation time (τ_D^β)	Enthalpy recovered (J/g)	Relaxation time (τ^β)
23 %	25 (12 h)	2.89±0.39	6.4±0.7 (0.22)	1.20±0.07	15.5±6.2 (0.54)
	30 (12 h)	3.53±0.10	2.9±0.1 (0.23)	1.51±0.11	10.2±1.3 (0.46)
	35 (6 h)	4.16±0.33	1.8±0.05 (0.24)	1.69±0.28	3.7±0.1 (0.39)
	40 (6 h)	2.04±0.03	1.6±0.02 (0.31)	*n.d.*	*n.d.*

n.d., not determined

The time in parenthesis is the time point for comparison of enthalpy relaxation and recovery. Data are average of three replicates for TAM and two for MDSC

seems to also measure some faster motions that occur well below the Tg [38–40]. Here, we extend such studies to more complex multicomponent spray dried carbohydrate matrices (Table 1).

Representative plots displaying the fits of the KWW equation for MDSC and the MSE derivative equation for TAM relaxation rate data are shown in Figs. 1 and 2 respectively. Tables 3 and 4 compare the relaxation times (τ^β) obtained from MDSC derived data with the corresponding data obtained from isothermal calorimetry for 50 % sucrose at 23 and 33 % RH, at different temperatures. The standard error reported is calculated from the reproducibility for two independent measurements for scanning calorimetry and for three independent measurements for isothermal microcalorimetry. As is evident from both the tables, the relaxation times at temperatures below the glass transition were significantly higher for scanning calorimetry (MDSC) compared to those obtained from isothermal microcalorimetry. This suggests that the relaxation times depend on the technique used, as found previously for simple one component systems. Note that the difference between the relaxation times obtained from the two methods increases at lower temperatures.

The values of enthalpy recovery (from MDSC) were then compared to enthalpy relaxed (from integrated TAM data) (Tables 3 and 4). Nominally, these values are the same if the same processes are being studied. To obtain the enthalpy recovered from DSC data, the non-reversing heat flow endothermic peak for the sample undergoing the longest annealing time was integrated. The enthalpy relaxed as measured by TAM data was obtained by integrating the power-time curve for the same time interval used in aging the sample studied by MDSC. The integration from time zero to 1 h, where reliable TAM data could not be obtained, was determined from integrating the MSE power equation with the fitted relaxation parameters. As seen from Table 3, the enthalpy relaxation from TAM is significantly larger than the enthalpy recovery values in nearly all cases. Higher relaxation values were also seen for 50 % sucrose, 33 % RH although the differences between enthalpy recovered and relaxed were relatively small. The enthalpy recovery is determined only by the overshoot enthalpy at or near the glass transition. Any transitions that occur below that representing relaxation or recovery are not included in DSC measurements. But TAM, however, measures everything relaxing at the temperature of the measurement. Therefore, the difference in the relaxed and the recovered values indicates that some relaxation is being measured by the TAM experiment which is not being measured by the enthalpy recovery measured as the system passes through the glass transition region. It seems likely that some fast beta-like relaxation or faster relaxing component of the alpha

Table 4 Comparison between calorimetric relaxation times (in hours) and beta values in parenthesis, obtained from isothermal microcalorimetry and modulated DSC along with enthalpy relaxation and recovery obtained at four temperatures for 50 % Sucrose at 33 %RH

% RH	Temperature (°C)	Isothermal microcalorimetry (MSE)		Modulated DSC (KWW)	
		Enthalpy relaxed (J/g)	Relaxation time (τ_D^β)	Enthalpy recovered (J/g)	Relaxation time (τ^β)
33 %	10 (12 h)	2.36±0.30	10.1±0.9 (0.41)	1.04±0.16	41.5±8.2 (0.75)
	15 (12 h)	2.52±0.32	5.5±0.3 (0.34)	2.13±0.28	10.2±0.8 (0.58)
	20 (8 h)	2.37±0.27	3.5±0.2 (0.30)	2.52±0.06	2.8±0.3 (0.42)
	25 (4 h)	1.61±0.16	1.8±0.1 (0.21)	2.16±0.11	1.9±0.2 (0.34)

The time in parenthesis is the time point for comparison of enthalpy relaxation and recovery. Data are average of three replicates for TAM and two for MDSC
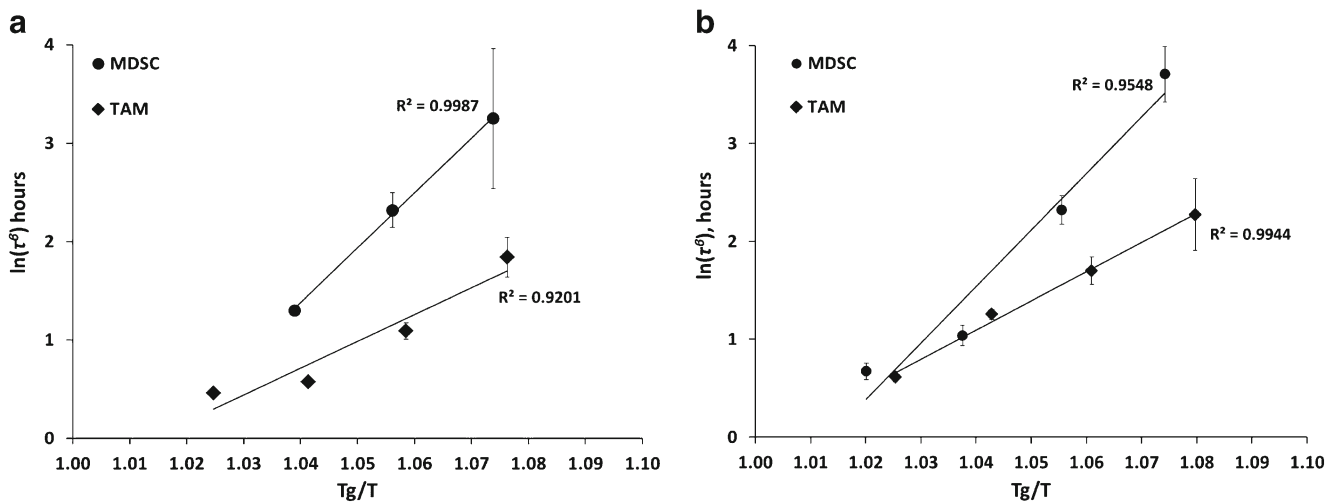
Fig. 3 Relaxation times as a function of the reciprocal of temperature for 50 % Sucrose. (**a**) 23 %RH and (**b**) 33 %RH

distribution is being measured by TAM, but this part of the relaxation is being recovered before the system passes through the glass transition region, as suggested by Bhugra and co-workers [38–40].

When the relaxation times for 50 % sucrose (23 % RH and 33 % RH) were plotted as a function of the reciprocal of temperature (Fig. 3), relaxation times derived from DSC and TAM techniques appear to converge at the glass transition. However, as the difference between the annealing and the glass transition temperature increases (i.e. as we approach lower temperatures) the relaxation data diverge.

The values of β evaluated from TAM were smaller (about 0.2) than the corresponding data obtained by KWW analysis of the DSC data 0.3–0.7) (Tables 3 and 4), as noted in previous work [30, 37]. However, as briefly discussed earlier the value of β obtained by either analysis is too small as a result of the changes in relaxation time during the measurements. Since the TAM procedure allows characterization of relaxation times at the lower temperatures in the range of most interest for our studies, further relaxation studies on blank matrices of 50 and 30 % sucrose were conducted using the TAM.

Effects of Relative Humidity and Temperature on Relaxation Times as Determined from Isothermal Microcalorimetry

All relaxation times for 50 and 30 % sucrose systems measured with isothermal microcalorimetry are reported in Tables 5 and 6, respectively. The tables also include the glass transition temperatures measured using modulated DSC. The relaxation time τ_D^β is a measure of the time required for motion on a large length scale (i.e., global mobility). An increase in enthalpy relaxation time suggests a decrease of free volume and a decrease of molecular mobility [41–44].

The relaxation time data were determined in the temperature region beginning 20 K below T_g and increasing in 5 K increments towards T_g for both the matrices. In some cases, relaxation studies were also performed for temperatures less than T_g -20 K in order to compare with the stability studies. Since increasing residual water plasticizes amorphous solids, lowering the T_g, we expect a decrease in relaxation time with water addition and a decrease in stability. This trend is largely followed for the 50 and 30 % sucrose systems when relaxation times at the same temperature are compared (Tables 5 and 6).

Table 5 Isothermal Microcalorimetric relaxation time in hours (± Standard Error) for 50 % Sucrose at different temperatures and four (11, 23, 33 and 43 %) relative humidities

11 %RH (T_g: 55.3)		23 %RH (T_g: 47.7)		33 %RH (T_g: 32.6)		43 %RH (T_g: 25.9)	
Temperature (°C)	Relaxation time (τ_D^β)	Temperature (°C)	Relaxation time (τ_D^β)	Temperature (°C)	Relaxation time (τ_D^β)	Temperature (°C)	Relaxation time (τ_D^β)
30	6.0 (*n*=1)	25	6.4±0.7	10	10.1±0.9	10	4.5±0.6
35	4.7±0.2	30	2.9±0.1	15	5.5±0.3	15	2.6±0.1
40	2.9±0.3	35	1.8±0.05	20	3.5±0.2	20	1.6±0.2
45	2.6±0.3	40	1.6±0.02	25	1.8±0.1	25	2.1±0.03
50	1.8±0.02			30	1.3 (*n*=1)		

Table 6 Isothermal microcalorimetric relaxation time in hours (± Standard Error) for 30 % sucrose at different temperatures and four (11, 23, 33 and 43 %) relative humidities

11 %RH (T_g: 66.3)		23 %RH (T_g: 57.1)		33 %RH (T_g: 49.8)		43 %RH (T_g: 42.8)	
Temperature (°C)	Relaxation time (τ_D^β)	Temperature (°C)	Relaxation time (τ_D^β)	Temperature (°C)	Relaxation time (τ_D^β)	Temperature (°C)	Relaxation time (τ_D^β)
30	34.1±7.2	30	40.6 ($n=1$)	25	9.2±1.2	20	3.5±0.7
40	15.4±3.1	35	13.9±0.6	30	4.6±0.2	25	3.7±0.6
45	9.9±0.8	40	8.5±0.6	35	3.2±0.06	30	2.1±0.1
50	8.4±0.6	45	5.9±0.5	40	2.6±0.04	35	1.3±0.1
55	4.8±0.4	50	4.2±0.1	45	1.4±0.03		
60	2.4±0.6						

The exceptions are likely a result of insufficient precision in the data to allow a meaningful comparison. If the major impact of differences in residual water on relaxation time arises through changes in T_g, one might expect that the temperature dependence of relaxation time for a given matrix would be a universal function of T_g/T. When the relaxation times for 50 and 30 % sucrose are plotted against the "normalized temperature, T_g/T, (Fig. 4), it is clear that not all data fall on a single curve. Thus, as fundamental considerations suggest [21, 45], factors other than T_g are also important in determining relaxation time. However, as a first approximation, the 11 and 23 % RH data seem to fall on a single curve as do the 33 and 43 % RH data. Since T_g is a function of water content, there should be a correlation of relaxation times with respect to the water content determined for each system at specific RH. In fact, if one restricts the data to systems studied at the same temperature, the correlation between relaxation dynamics and water content is similar to the correlation shown in Fig. 4 for relaxation dynamics as a function of T_g/T at fixed relative humidity. However, if all data are included, the correlation between relaxation dynamics and water content is extremely poor, as

expected since temperature is a major variable in determining relaxation time. However, using all data the correlation coefficient between relaxation dynamics and T_g/T is rather good, 0.68 and 0.82 for 30 and 50 % Sucrose, respectively.

Correlation of Stability with Structural Relaxation Times

Generally, there are two broad classes of dynamics in glasses; primary relaxation (α-relaxation or the structural relaxation) and secondary relaxations (β-relaxation, Johari-Goldstein relaxation, and others) [18, 46]. Primary relaxation reflects the global mobility of the whole molecule or groups of atoms over a long length scale and long time scales, which is highly cooperative motion. α-relaxation is directly coupled to viscosity. Secondary relaxations reflect the local mobility over short length scales and over much shorter time scales. This motion is not highly cooperative. A decrease in the molecular mobility is expected to decrease the degradation rate (k); and therefore one might expect a relationship of the form,
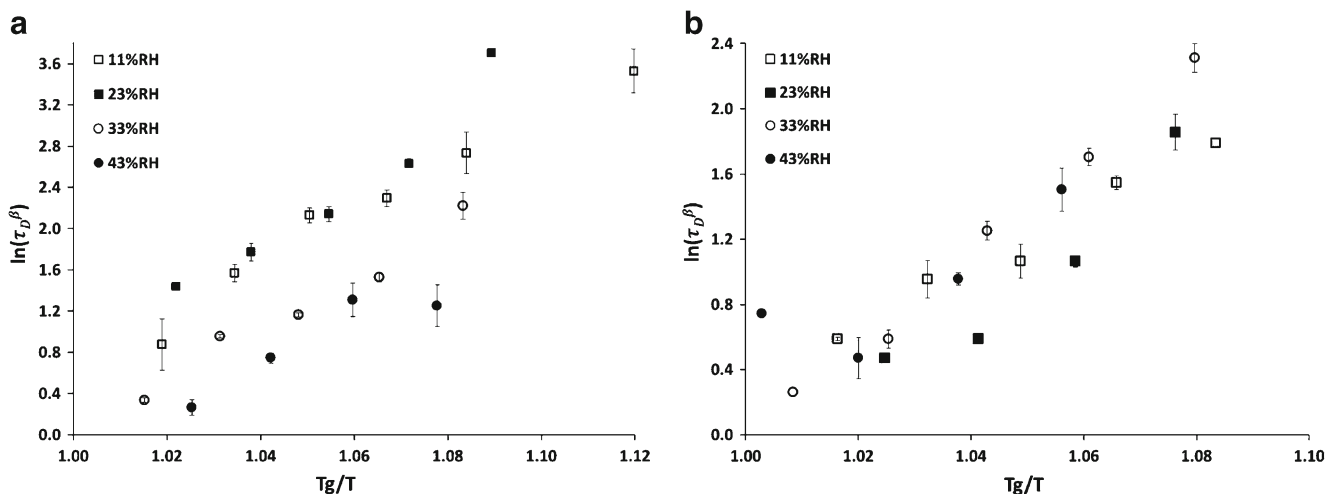
$$k \propto (mobility)^c \tag{6}$$

Fig. 4 Effect of relative humidity on the relaxation times as a function of normalized temperature, T_g/T, for **a** 30 % Sucrose and **b** 50 % Sucrose

Table 7 Degradation rate constants for loss of volatiles (Methyl acetate , Ethyl acetate & Limonene) and formation of oxidation byproducts for 50 % sucrose following time (week) kinetics. With some entries, low error allows more significant figures in the k

%RH	T	T/Tg	(τ_D^β)	$\log(1/\tau_D^\beta)$	k_{MeOAc} ($\sqrt{t}$)	k_{EtOAc} ($\sqrt{t}$)	$k_{Limonene}$ ($\sqrt{t}$)	k_{OxBP} (t)
11 %RH	40	0.95	2.9±0.3	−0.47	n.d.	0.016±0.004	0.005±0.002	n.d.
	30	0.92	6.0 (n=1)	−0.78	n.d.	0.007±0.003	n.d.	n.d.
23 %RH	40	0.98	1.59±0.02	−0.20	n.d.	0.020±0.005	0.008±0.001	n.d.
	30	0.94	2.9±0.1	−0.47	0.026±0.004	0.026±0.008	0.006±0.002	n.d.
33 %RH	40	1.02	n.d.		0.212±0.014	0.11±0.02	0.036±0.003	0.020±0.005
	30	0.99	1.3 (n=1)	−0.09	0.073±0.007	0.05±0.01	0.018±0.003	0.010±0.003
43 %RH	40	1.05	n.d.		0.47±0.26	0.34±0.10	0.059±0.006	n.d.
	30	1.01	n.d.		0.45±0.19	0.29±0.05	0.054±0.006	n.d.

n.d., not determined

where the coupling coefficient c, of unity shows perfect coupling as would result from a diffusion controlled reaction in which the translational diffusion coefficient is inversely related to viscosity according to the Stokes-Einstein equation. Consequently, if the motion involved in the degradation process is closely related to the motion measured by the structural relaxation time, degradation rate is correlated or strongly coupled to structural relaxation (i.e., c≈1), and the rate of structural relaxation on the "stretched time scale" (τ^β) is the significant kinetic parameter when degradation and relaxation processes are compared [13, 46, 47].

The kinetics of loss of volatiles is likely controlled by diffusion of the molecule through the glassy phase or perhaps evaporation at the solid-vapor boundary [48]. What controls the rate of oxidation is less obvious, but since any chemical reaction will require movement of molecules or groups of atoms, such as diffusion of reactive oxygen species in the glass or movement of groups of atoms through the transition state, one might expect a correlation between the rate constant for the reaction and mobility of the glass matrix, as measured by relaxation time. In glassy systems, the degradation rate is often observed to follow "square root in time" kinetics; that is,

for a small amount of degradation, the accumulation of degradation product is proportional to the square root of time. This is an empirical observation, valid for a wide variety of glassy systems, but does have a foundation in theory [46]. We would expect loss of volatiles (methyl acetate, ethyl acetate and limonene) to be diffusion controlled, which means loss of mass, m, from the initial value, m_0, is given by

$$m(t) = m_0 - k\, m_0 \sqrt{t} + m_0 O(t) \qquad (7)$$

where m is the mass at time t, m_o is the initial mass, k is the rate constant, $O(t)$ denotes higher order terms which are small at small times [48].

Further, the percent of degradation products via oxidation, $\% D$, may be written in the form,

$$\%D = D_0 + kt^n \qquad (8)$$

where D_0 is the initial level of degradant, k is the apparent rate constant, and n is usually 0.5 in amorphous pharmaceutical glasses [45]. However, multiple linear regressions was

Table 8 Degradation rate constants for loss of volatiles (Methyl acetate , Ethyl acetate & Limonene) and formation of oxidation byproducts for 30 % sucrose following time (week) kinetics. With some entries, low error allows more significant figures in the k

%RH	T	T/Tg	(τ_D^β)	$\log(1/\tau_D^\beta)$	k_{MeOAc} ($\sqrt{t}$)	k_{EtOAc} ($\sqrt{t}$)	$k_{Limonene}$ ($\sqrt{t}$)	k_{OxBP} (t)
11 %RH	40	0.92	15.4±3.1	−1.19	0.045±0.009	0.022±0.012	0.019±0.003	0.020±0.003
	30	0.89	34.1±7.2	−1.53	n.d.	0.024±0.008	0.010±0.003	0.014±0.003
23 %RH	40	0.95	8.5±0.6	−0.93	n.d.	0.028±0.008	0.025±0.003	0.024±0.003
	30	0.92	40.6 (n=1)	−1.61	n.d.	0.034±0.011	0.015±0.004	0.016±0.004
33 %RH	40	0.97	2.63±0.04	−0.42	0.052±0.012	0.049±0.022	0.045±0.003	0.031±0.005
	30	0.94	4.6±0.2	−0.66	0.027±0.005	0.040±0.010	0.029±0.003	0.024±0.003
43 %RH	40	0.99	n.d.		0.33±0.03	0.196±0.012	0.114±0.003	0.088±0.045
	30	0.96	2.1±0.1	−0.33	0.20±0.04	0.082±0.006	0.069±0.008	0.058±0.016

n.d. not determined

Fig. 5 Coupling between the log of inverse relaxation time (τ_D^β) and log rate constants for the loss of Methyl and Ethyl Acetate at temperatures below the glass transition temperatures for the same T_g/T. The lines represent the linear regression of the data for 50 % Sucrose, Loss of EtOAc, $R^2=0.77$, log (k)=1.00 log ($1/\tau_D^\beta$) − 1.30 For loss of MeOAc, the two data points are in a ratio consistent with a coupling coefficient of unity
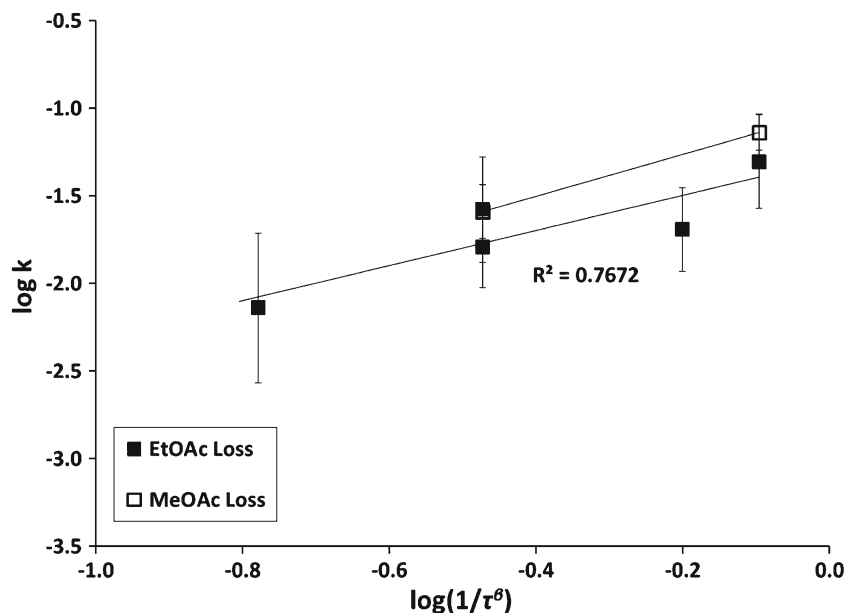

executed in order to fit the most pertinent model (with varying exponents or *n* values, 0.5 & 1 in Eq. 8) to the assay data points for both the matrices. In order to determine the most appropriate model, a statistical analysis was conducted by computing F-values for both 30 and 50 % sucrose matrices. The F values (data not included) for $n=1$ were significantly greater than for $n=0.5$, typically by an order of magnitude. Hence, the oxidation degradation assay data analyzed from Eq. 8 with $n=1$ are reported here. It should be noted that the analysis with $n=0.5$ gives essentially the same results in the comparison of degradation rate constant with structural relaxation time.

The degradation data included here are somewhat limited in scope. We did investigate other conditions but the low level of degradation that developed was insufficient to provide quantitative rate constant data that would allow a meaningful comparison with relaxation times. Thus, any rate constants with standard errors in excess of ½ the values of the rate constant were not included. In particular, this meant a sparse data set at low humidities and low temperatures.

Rate constants (for loss of volatiles and formation of oxidation products) and the τ_D^β values are compared at 30 and 40 °C for 50 and 30 % sucrose systems in Tables 7 and 8 in Figs. 5, 6 and 7. An increase in the relative humidity and the corresponding increase in water content results in a moderately higher loss of volatiles (methyl acetate, ethyl acetate and limonene) for both 50 and 30 % sucrose systems (Tables 7 and 8). Loss of volatiles, as expected, is generally significantly

Fig. 6 Coupling between the log of inverse relaxation time (τ_D^β) and log rate constants for the loss of limonene at temperatures below the glass transition temperatures for the same T_g/T. The lines represent the linear regression of the data. (For 30 % Sucrose, $R^2=$ 0.91, log (k)=0.52 log ($1/\tau_D^\beta$) − 1.10 and for 50 % Sucrose, $R^2=$ 0.80, log (k)=1.11 log ($1/\tau_D^\beta$) − 1.74
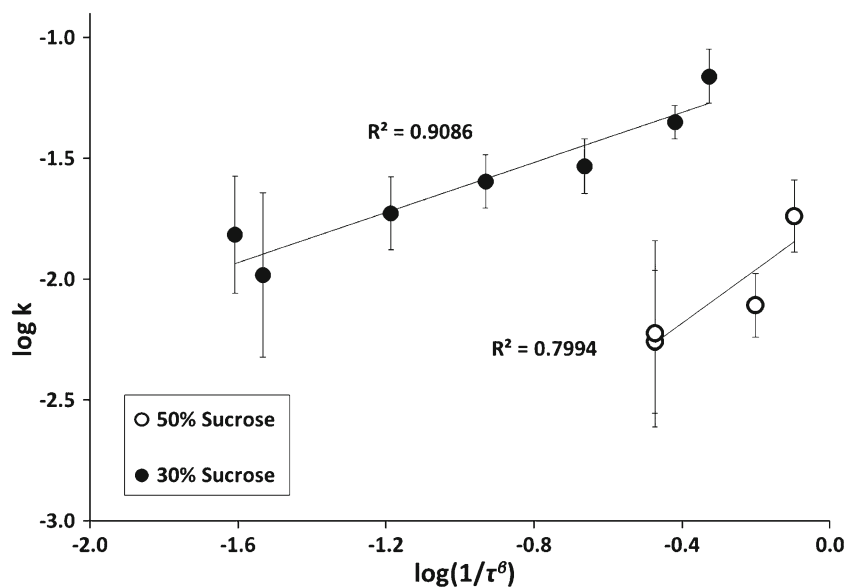
higher at higher temperatures. The trends for rate constants in 30 and 50 % Sucrose follow the order of methyl acetate≥ethyl acetate>limonene. This trend may be due, in part, to higher boiling point and therefore lower vapor pressure of Limonene (176 °C) compared to Ethyl Acetate (77.1 °C) and Methyl acetate (56.9 °C, with highest volatile loss), but may also be attributed in part to the differences in molecular size. Moreover, in spite of a lower T_g in the 50 % Sucrose system, stability against loss of limonene was somewhat better with the 50 % sucrose matrix.

Oxidation is slightly greater at higher relative humidity conditions. The increased oxidation rate at higher relative humidity is due to increased oxygen mobility through the matrix, which is expected as the system approaches Tg due to increased plasticization at high RH. Due to the difficulty in accurately measuring small limonene oxidation rates, there is only a single data set for 50 % sucrose. Judging only from this point, the higher sucrose content provided better protection against oxidation, as demonstrated for 33 % RH data from Tables 7 and 8, although the difference here is small. However this same trend is often observed in shelf stability tests of spray dried delivery systems. Note also that higher enthalpy relaxation time (lower mobility) resulted in a better protection against oxidation (Table 8).

Figs. 5, 6 and 7 explore the correlation between stability and structural relaxation time in more detail, where log-log plots of the rate constant for loss of volatile or oxidation versus the inverse of the relaxation time ($1/\tau_D{}^\beta$) are given. The coupling coefficient for loss of Ethyl Acetate, Methyl Acetate and Limonene for 50 % sucrose was found to be unity as shown in Figs. 5 and 6. However, the coupling coefficient for the loss of limonene were found to be somewhat lower (0.52±0.07) for 30 % sucrose, as shown in Fig. 6, where the uncertainty

represents standard error. As mentioned earlier, a coupling coefficient of unity suggests a diffusion controlled reaction, which in case of loss of volatiles is expected, and lower values indicate that the motions required for degradation are weakly coupled to the motions concerned with structural relaxation. For degradation by oxidation (Fig. 7), correlation between rate constant and relaxation time is quite good, but the coupling coefficient is somewhat lower at 0.36±0.12, suggesting that the motions required for oxidative degradation are more weakly coupled to the motions measured by structural relaxation, although the difference is within the sum of the standard errors. Typically, similar attempts to correlate degradation rates in pharmaceutical systems with relaxation time give coupling coefficients less than unity [45, 47]. A coupling coefficient greater than zero but significantly less than unity suggests that the motion involved in the degradation is not as highly cooperative as the motion involved in relaxation (and does not demand as much "free volume" to pass through the transition state). A chemical reaction, such as oxidation, likely involving diffusion of a small reactive oxygen species in a system of larger molecules (sucrose) or motion of several atoms in going through the transition state would not be expected to have the same demands for creation of free volume. Thus, a coupling coefficient less than unity is expected. Despite the uncertainty involved in the coupling coefficient results, the data suggest significant coupling between the degradation rate constants and the structural relaxation measurements for both the systems. There exists a qualitative correlation between larger relaxation time and greater stability for loss of methyl and ethyl acetate for 30 % sucrose.

We note that mobility in the glassy system could well limit oxidation kinetics even without being dependent on the diffusion rate of oxygen. After all, atoms and groups of atoms need

Fig. 7 Coupling between the log of inverse relaxation time (τ_{D^β}) and log rate constants for formation of oxidation byproducts at temperatures below the glass transition temperatures for the same T_g/T. The lines represent the linear regression of the data. (For 30 % Sucrose, $R^2 = 0.81$, $\log(k) = 0.36 \log(1/\tau_{D^\beta}) - 1.28$)
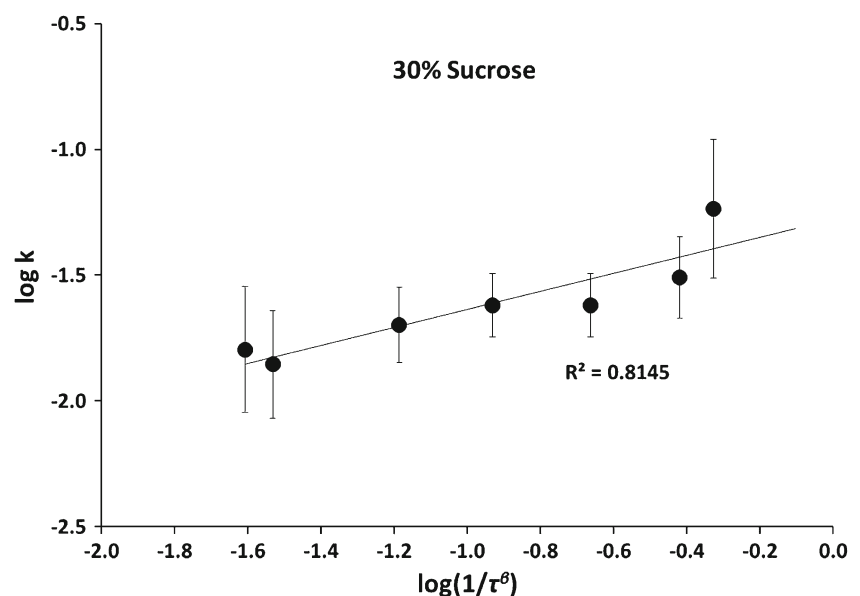
to move into and through the transition state in "diffusion-like" motion to complete the reaction. Thus, mobility of at least some kind may be relevant even in an oxidation reaction that is not controlled by the rate of oxygen diffusion. With that stated, however, previous studies of the oxidation rate of oil incorporated in similar glassy matrices composed mostly of sucrose and maltodextrin found that the overall oxidation rate seemed to be limited by the rate of diffusion of Oxygen through the matrix surrounding the droplets of oil at $T < T_g$ and room temperature or above [49–51], which is consistent with our interpretation. We have no information about how the effective solubility of Oxygen in the glassy matrix changes as a function of water content and matrix composition. As a first approximation we have assumed that the solubility is unaffected. In further studies, it would be desirable to find means of measuring the extent and rate of Oxygen uptake into the matrix more directly.

Conclusions and Significance

It is extremely important to recognize which mobility substate is accountable for the instability of interest. In the current work, relaxation times were measured for temperatures below the glass transition temperature for different amorphous systems using modulated and isothermal calorimetric techniques. It was observed that the relaxation times are very much dependent on the technique used, although that does not necessarily mean that qualitative trends change with the technique. A comparison of the relaxation times from both the techniques suggests that the isothermal calorimeter is capturing some of the faster dynamics as well as the dynamics that are activated near T_g. Further, a correlation between the relaxation times and the degradation constants obtained from loss of volatiles and formation of oxidation byproducts is established. In general, when accuracy of the data permits comparison, greater stability for both oxidation and loss of volatiles is well correlated with longer structural relaxation time.

References

1. S. Gouin, Trends Food Sci. Technol. **15**, 330–347 (2004)
2. J. Ubbink, A.M. Schoonman, Flavor delivery systems, in *Kirk-Othmer Encyclopedia of Chemical Technology*, ed. by S. Azra (Wiley, New York, 2005), pp. 527–563
3. L. Doorn, F. Campanile Gum s and Stabilisers for the Food Industry (2006), pp. 268–274
4. M. Porzio, Food Technol. **66**, 52–64 (2012)
5. G.A. Reineccius, Dry. Technol. **22**, 1289–1324 (2004)
6. S. Anandaraman, G.A. Reineccius, Food Technol. **40**, 88–93 (1986)
7. W. Baisier, G.A. Reineccius, Perfumer & Flavorist **14**, 48–53 (1989)
8. R.L. Anaandaraman, A. Vaezy, A. Schober, Y. Rada, R.M.T.V. Rong, R. Sleeuwen, S. Golding, V. Zhang, Normand. Carbohydr. Polym. **97**, 352–357 (2013)
9. Y.M. Gunning, R. Parker, S.G. Ring, Carbohydr. Res. **329**, 377–385 (2000)
10. D.W. Bohn, K.R. Cadwallader, S.J. Schmidt, J. Food Sci. **70**, E109–E116 (2005)
11. D. Kilburn, J. Claude, T. Schweizer, A. Alam, J. Ubbink, Biomacromolecules **6**, 864–879 (2005)
12. S. Townrow, D. Kilburn, A. Alam, J. Ubbink, J. Phys. Chem. B **111**, 12643–12648 (2007)
13. S.A. Luthra, I.M. Hodge, M. Utz, M.J. Pikal, J. Pharm. Sci. **97**, 5240–5251 (2008)
14. B. Wang, M.J. Pikal, J. Pharm. Sci. **99**, 663–682 (2010)
15. B. Wang, M.T. Cicerone, Y. Aso, M.J. Pikal, J. Pharm. Sci. **99**, 683–700 (2010)
16. S.A. Luthra, E.Y. Shalaev, A. Medek, J. Hong, M.J. Pikal, J. Pharm. Sci. **101**, 3110–3123 (2012)
17. N. Chieng, M. Mizuno, M.J. Pikal, Eur. J. Biopharm. **85**, 189–196 (2013)
18. N. Chieng, M.T. Cicerone, Q. Zhong, M. Liu, M.J. Pikal, Eur. J. Biopharm. **85**, 197–206 (2013)
19. L.C.E. Struik, *Physical aging in amorphous polymers and other materials* (Elsevier Scientific Pub. Co, Amsterdam, 1978)
20. B.C. Hancock, S.L. Shamblin, G. Zografi, Pharm. Res. **12**, 799–806 (1995)
21. I.M. Hodge, J. Non-Cryst. Solids **169**, 211–266 (1994)
22. D.Q.M. Craig, M. Barsnes, P.G. Royall, V.L. Kett, Pharm. Res. **17**, 696–700 (2000)
23. D.J. Hourston, M. Song, A. Hammiche, H.M. Pollock, M. Reading, Polymer **37**, 243–247 (1996)
24. A.M. Lammert, R.M. Lammert, S.J. Schmidt, J. Therm. Anal. Calorim. **55**, 949–975 (1999)
25. A. Alegria, A. Goitiandia, I. Telleria, J. Colmenero, Macromolecules **30**, 3881–3887 (1997)
26. F. Badii, C. Martinet, J.R. Mitchell, I.A. Farhat, Food Hydrocoll. **20**, 879–884 (2006)
27. H.J. Chung, B. Yoo, S.T. Lim, Starch **57**, 354–362 (2005)
28. K.L. Ngai, D.J. Plazek, Rubber Chem. Technol. **68**, 376–434 (1995)
29. C.M. Roland, K.L. Ngai, Macromolecules **24**, 2261–2265 (1991)
30. K. Kawakami, M.J. Pikal, J. Pharm. Sci. **94**, 948–965 (2005)
31. P. Tong, G. Zografi, Pharm. Res. **16**, 1186–1192 (1999)
32. B.C. Hancock, S.L. Shamblin, Thermochim. Acta **380**, 95–107 (2001)
33. Y.T. Liu, B. Bhandari, W.B. Zhou, J. Agric. Food Chem. **54**, 5701–5717 (2006)
34. S.L. Shamblin, B.C. Hancock, Y. Dupuis, M.J. Pikal, J. Pharm. Sci. **89**, 417–427 (2000)
35. Z. Jiang, C.T. Imrie, J.M. Hutchinson, J. Therm. Anal. Calorim. **64**, 85–107 (2001)
36. S. Weyer, A. Hensel, C. Schick, Thermochim. Acta 304 Y305:267 Y 275 (1997)
37. J. Liu, D.R. Rigsbee, C. Stotz, M.J. Pikal, J. Pharm. Sci. **91**, 1853–1862 (2002)
38. C. Bhugra, R. Shmeis, S.L. Krill, M.J. Pikal, Pharm. Res. **23**, 2277–2290 (2006)
39. C. Bhugra, S. Rambhatla, A. Bakri, S. Duddu, D. Miller, M. Pikal, D. Lechuga-Ballesteros, J. Pharm. Sci. **96**, 1258–1269 (2007)
40. C. Bhugra, R. Shmeis, S.L. Krill, M.J. Pikal, J. Pharm. Sci. **97**, 455–472 (2008)
41. S. Montserrate, J. Appl. Polym. Sci. **44**, 545–554 (1992)
42. H.J. Chung, S.T. Lim, Food Hydrocoll. **17**, 851–861 (2003)
43. H.J. Chung, S.T. Lim, Starch-Starke **58**, 599–610 (2006)

44. H.J. Chung, H.I. Chang, S.T. Lim, Carbohydr. Polym. **58**, 101–107 (2004)
45. S.L. Shamblin, B. Hancock, M.J. Pikal, Pharm. Res. **23**, 2254–2268 (2006)
46. L. Chang, D. Shepherd, J. Sun, D. Ouellette, K.L. Grant, X. Tang, M.J. Pikal, J. Pharm. Sci. **94**, 1427–1444 (2005)
47. M.J. Pikal, D. Rigsbee, M.L. Roy, D. Galreath, K.J. Kovach, B. Wang, J.F. Carpenter, M.T. Cicerone, J. Pharm. Sci. **97**, 5106–5121 (2008)
48. M.J. Pikal, S. Shah, Int. J. Pharm. **62**, 165–186 (1990)
49. V. Orlien, A.B.. Andersen, T. Sinkko, L.H. Skibsted, Food Chem. **68**, 191–199 (2000)
50. A.B.. Andersen, J. Risbo, M.L. Andersen, L.H. Skibsted, Food Chem. **70**, 499–508 (2000)
51. V. Orlien, J. Risbo, H. Rantanen, L.H. Skibsted, Food Chem. **94**, 37–46 (2006)